Heavy-Flavor Production at RHIC with STAR

Zhenyu Ye (for the STAR Collaboration)

University of Illinois at Chicago, Chicago, Illinois 60607, USA
Central China Normal University, Wuhan 430079, China

Abstract. Heavy-flavor particles have been suggested as an excellent probe to study properties of the Quark-Gluon Plasma, a new state of matter discovered in high-energy heavy-ion collisions. In these proceedings, we report a few highlighted results on heavy-flavor production from the STAR experiment, including the first physics results obtained with the newly installed Heavy Flavor Tracker for open heavy flavor and the Muon Telescope Detector for quarkonium studies. These results are compared to results from other experiments and theoretical calculations, and the physics implications are also discussed.

1. Introduction

Through measurements of heavy-flavor production, we can study parton interactions with the Quark-Gluon Plasma (QGP) and thus the properties of the QGP. Measurements of open heavy flavor hadrons and quarkonia at the Relativistic Heavy Ion Collider (RHIC) have revealed very interesting features, such as enhancement (suppression) of open charm hadron production at intermediate (high) transverse momentum (p_T) in Au+Au collisions compared to p+p collisions at $\sqrt{s_{NN}} = 200$ GeV [1], small beam energy dependence of J/ψ suppression integrated over p_T in Au+Au collisions from $\sqrt{s_{NN}} = 39$ to 200 GeV [2]. The former can be described by theoretical calculations with strong charm-QGP interactions as well as charm-light quark coalescence, while the latter can be understood by taking into account both the color screen effect and regeneration of J/ψ from uncorrelated $c\bar{c}$ pairs.

Many progresses have been made on this front, but there are still important questions not fully addressed, such as how parton-QGP interactions depend on the flavor and mass of the partons, and how the properties of the QGP depend on its temperature. More precise measurements at RHIC are needed to answer these questions. The STAR experiment has recently completed data taking with two new detectors for heavy-flavor studies, the Heavy Flavor Tracker (HFT) [3] and Muon Telescope Detector (MTD) [4]. In these proceedings, we report recent results from STAR on heavy-flavor production, including the first physics results from the HFT and MTD.

2. STAR Experiment

STAR is a large acceptance, multi-purpose detector at RHIC designed to study the QGP. Enclosed in a 0.5 Tesla solenoidal magnet are a Time Projection Chamber (TPC), a Time-Of-Flight detector (TOF), and a Barrel ElectroMagnetic Calorimeter (BEMC). The TPC is the main tracking detector for STAR. It also provides particle identification capability through measurement of the specific energy loss (dE/dx). The TOF greatly improves particle identification at low p_T. The BEMC is used to trigger on and identify high-p_T electrons. These detectors cover full azimuth over a large pseudo-rapidity range ($|\eta| < 1$).

Since the beginning of 2014, two new detectors, the HFT and MTD, have been fully integrated into STAR. The HFT consists of four layers of silicon detectors, located inside the TPC. With thinned Monolithic Active Pixel Sensors (MAPS), the HFT provides excellent track impact parameter resolution even at p_{T} down to 0.2 GeV/c for open heavy flavor measurements. The MTD installed outside of the solenoidal magnet is based on the Multi-gap Resistive Plate Chamber (MRPC) technology. With precise time-of-flight information, the MTD can trigger on and identify muons with $p_{\mathrm{T}} > 1.2$ GeV/c and $|y| < 0.5$. The HFT and MTD have recorded significant amount of data in p+p, p+Au, d+Au, and Au+Au collisions at $\sqrt{s_{\mathrm{NN}}} = 200$ GeV in 2014-2016. Results presented below are obtained from around 1/4 of the Minimum-Bias (MB) data with the HFT and 1/2 of the dimuon trigger data with the MTD in Au+Au collisions.

3. Open Heavy Flavor Production

The total charm production cross-sections at mid-rapidity ($|y| < 1$) have been measured by STAR in p+p and Au+Au collisions at $\sqrt{s_{\mathrm{NN}}} = 200$ GeV, and are found to scale with the number of binary nucleon collisions (N_{bin}) [1]. This observation supports that heavy-flavor quarks are predominantly produced in initial hard parton scatterings at RHIC. Moreover, because of their relatively long lifetime, heavy-flavor quarks can experience the whole evolution of the system. Therefore, they can serve as calibrated probes to study the QGP. Below, we present results on open heavy flavor production through the hadronic and semi-leptonic decay channels.

3.1. D^0-Meson R_{AA} and v_2

The HFT can significantly improve the signal-to-background (S/B) ratio for open charm hadron reconstruction, leading to greatly reduced uncertainties for the measurements of the nuclear modification factor R_{AA}, which is defined as the ratio between the yield in Au+Au collisions and that in p+p collisions scaled by N_{bin}. Shown in the left panel of Fig. 1 are the D^0-meson R_{AA} in 0-10% Au+Au collisions at $\sqrt{s_{\mathrm{NN}}} = 200$ GeV extracted from about 780 million MB events with the HFT (black solid circles). Also shown are the STAR published results from 1.1 billion MB events recorded in 2010 and 2011 without the HFT (red open circles) [1]. The vertical bars (brackets) represent statistical (systematic) uncertainties, while the grey shaded areas p+p reference systematic uncertainties for the R_{AA} obtained from the HFT data. The latter were not present for the published results due to cancellation of efficiency corrections between the p+p and 2010/2011 Au+Au data, both of which did not have the HFT. The sizes of the boxes around $R_{\mathrm{AA}} = 1$ in the left panel correspond to global normalization uncertainties for 0-10% Au+Au (left) and $p+p$ (right) collisions. Despite using a smaller data sample, the HFT results have significantly better precision than the published results, confirming the strong suppression of the D^0-meson R_{AA} at high p_{T}. The HFT has also enabled the first v_2 measurements for open charm hadrons at RHIC. Shown in the middle panel of Fig. 1 are the D^0 v_2 in 0-80% Au+Au collisions extracted from the abovementioned data. The vertical bars (brackets) represent statistical (systematic) uncertainties, while the grey shaded areas estimate of non-flow effects. When plotted as a function of $(\sqrt{m_0^2 + p_{\mathrm{T}}^2} - m_0)/n_q$, where m_0 is the hadron mass and n_q the number of constituent quarks, the D^0 v_2/n_q is below those of light hadrons, but still consistent within uncertainties, suggesting non-zero charm quark flow [5].

The measured R_{AA} and v_2 are compared to theoretical calculations, which use different approaches to describe transportation or interaction of charm quarks in the medium (for details see [6] and the references therein). The TAMU model uses a non-perturbative T-matrix approach with potentials obtained from Lattice QCD calculations to describe two-body interactions. The SUBATECH model uses perturbative QCD to evaluate hard interactions and resummation with Hard Thermal Loop approximation for soft collisions. The DUKE model uses a generalized Langevin approach with transport coefficients tuned to LHC data. As shown in Fig. 1, the
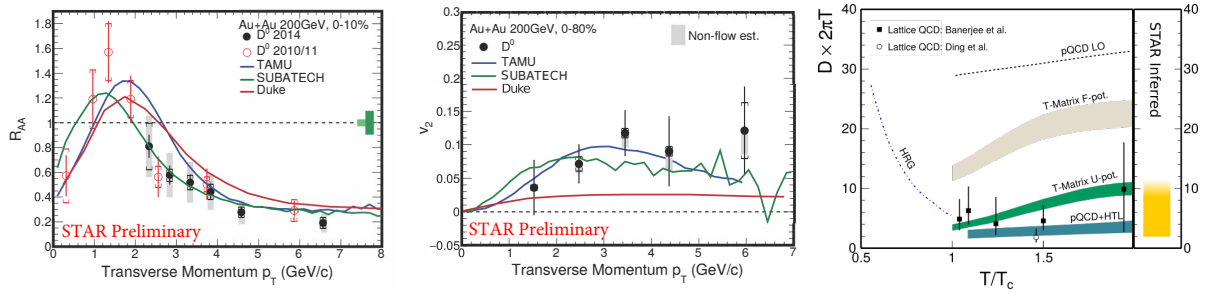
Figure 1. Left (middle): D^0 nuclear modification factor R_{AA} (elliptic flow v_2) in Au+Au collisions at $\sqrt{s_{NN}} = 200$ GeV. Right: charm quark diffusion coefficient. See text for details.
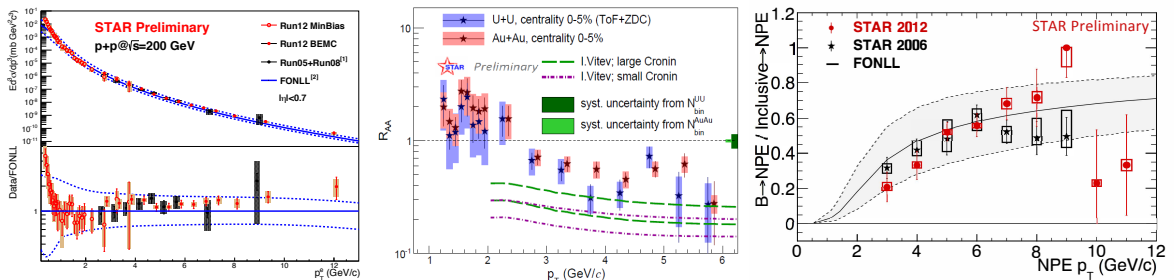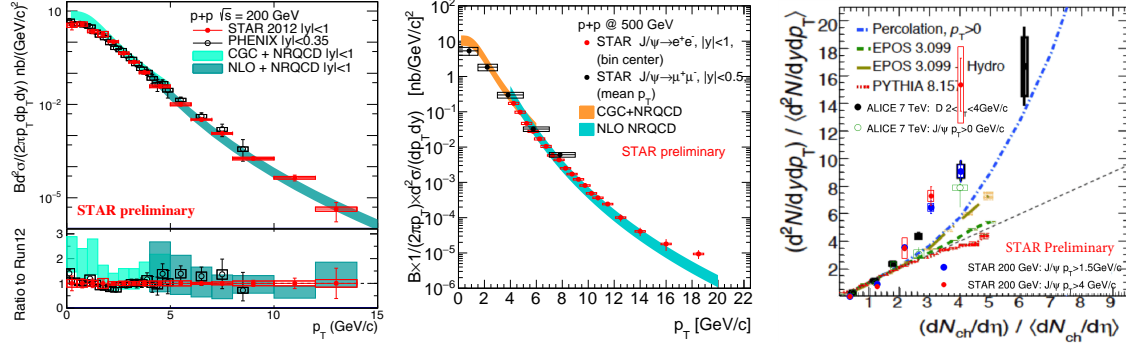

Figure 2. Left: e^{HF} cross-section in p+p collisions at $\sqrt{s} = 200$ GeV; Middle: e^{HF} R_{AA} in 0-5% Au+Au (U+U) collisions at $\sqrt{s} = 200$ (193) GeV; Right: relative contribution of bottom-decayed electrons in p+p collisions at $\sqrt{s} = 200$ GeV. See text for details.

TAMU and SUBATECH models describe both the R_{AA} and v_2, while the DUKE model describes the R_{AA} but underestimates the v_2. The charm quark diffusion coefficient $D \times 2\pi T$ extracted from the TAMU (SUBATECH) model ranges between 3-11 (2-4) for $T/T_c = 1$-2, shown as the green (blue) band in the right panel of Fig. 1, and agrees with Lattice QCD calculations [7].

3.2. Electrons from Semi-leptonic Decays of Open Heavy Flavor Hadrons

Heavy flavor production can also be studied through semi-leptonic decay channels. Using the data taken in 2010 and 2012, STAR has studied electrons from open heavy flavor hadron decays (e^{HF}) in p+p and Au+Au collisions at $\sqrt{s_{NN}} = 200$ GeV and U+U collisions at $\sqrt{s_{NN}} = 193$ GeV. The results are shown in Fig. 2, where the vertical bars (shaded areas or boxes) represent statistical (systematic) uncertainties. The 2012 p+p results (red circles) have much better precision and wider p_T coverage than the STAR published results from data taken in 2005 and 2006 (black circles) [8]. They agree with Fixed-Order-Next-to-Leading-Log (FONLL) predictions [9], with small tension at low p_T. Using this updated p+p reference, the e^{HF} R_{AA} in 0-5% Au+Au and U+U collisions are found to be consistent with each other. The LANL model using perturbative QCD to calculate parton-QGP interactions underestimates the measured R_{AA}.

In order to fully understand the parton-QGP interactions, we need to measure charm and bottom production separately. Shown in the right panel of Fig. 2 are the relative contributions from bottom hadron decays to e^{HF} in p+p collisions at $\sqrt{s} = 200$ GeV. They are determined by fitting the azimuthal correlation between e^{HF} and hadrons in data to the template distributions of charm- and bottom-decayed electrons extracted from PYTHIA, which have different shapes in the near-side peak due to different decay kinematics. Results obtained from the 2012 p+p data are consistent with the STAR published results from the 2006 data [10] and FONLL calculations [9]. Studies are underway to separate charm- and bottom-decayed electrons through their track impact parameters measured with the HFT in heavy-ion collisions.

Figure 3. Left (middle): J/ψ production cross-section in p+p collisions at $\sqrt{s} = 200$ (500) GeV; Right: relative J/ψ and D^0 yield versus charged-particle multiplicity in p+p collisions. The vertical bars (boxes) represent statistical (systematic) uncertainties. See text for details.
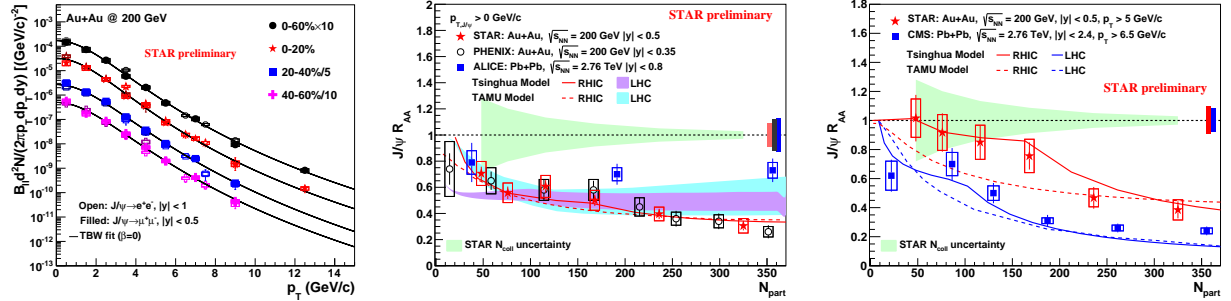
Figure 4. Left: J/ψ invariant yields in Au+Au collisions at $\sqrt{s_{NN}} = 200$ GeV; Middle: J/ψ R_{AA} for $p_T > 0$ GeV/c in Au+Au (Pb+Pb) collisions at $\sqrt{s_{NN}} = 200$ GeV (7 TeV); Right: J/ψ R_{AA} for $p_T > 5$ (6.5) GeV/c in Au+Au (Pb+Pb) collisions at $\sqrt{s_{NN}} = 200$ GeV (2.76 TeV). The vertical bars (boxes) represent statistical (systematic) uncertainties. See text for details.

4. Quarkonium Production

Quarkonia are made of bound heavy quark-antiquark pairs. While the heavy quark production can be calculated by pQCD, how they evolve into quarkonia are not fully known. Precise measurements of quarkonium production in p+p collisions can help understand the quarkonium production mechanisms. In heavy-ion collisions, quarkonia may dissociate due to the color screening of the heavy quark-antiquark potential in the QGP. Such dissociation depends on the temperature of the QGP and varies for different quarkonium states with different binding energies. Therefore, quarkonium production can be used to determine the QGP temperature once the color screening, regeneration, and cold nuclear matter effects are understood. Below, we present results on J/ψ and Υ productions in p+p, Au+Au and U+U collisions.

4.1. J/ψ Production in p+p Collisions

Differential cross-section of J/ψ production as a function of p_T has been measured in p+p collisions. Shown in the left panel of Fig. 3 are the STAR results (red circles) obtained from the 2012 data and PHENIX published results [11] (black circles) at $\sqrt{s} = 200$ GeV. They are consistent with each other, but the STAR results have much better precision at high p_T. Shown in the middle panel are the results at $\sqrt{s} = 500$ GeV from the dimuon (black circles) and dielectron channels (red circles). Both the 200 and 500 GeV results can be described by CGC+NRQCD calculations [12] at low p_T and NLO NRQCD calculations [13] at high p_T.

We have also studied how J/ψ production depends on charged-particle multiplicity (N_{ch}) in p+p collisions at $\sqrt{s} = 200$ GeV. As shown in the right panel of Fig. 3, a faster-than-

linear increase of relative J/ψ yield versus relative N_{ch} has been observed, suggesting not only correlation between soft and hard interactions, but also stronger suppression on soft interactions than hard interactions or stronger enhancement to hard interactions than soft interactions in high multiplicity p+p collisions. Such an increase is found to be independent of beam collisional energy when comparing these results with those at $\sqrt{s} = 7$ TeV [14]. The observed global trend independent of beam collisional energy is consistent with the Percolation model predication [15], but not with predications by the EPOS3 event generator with hydrodynamic evolution [16].
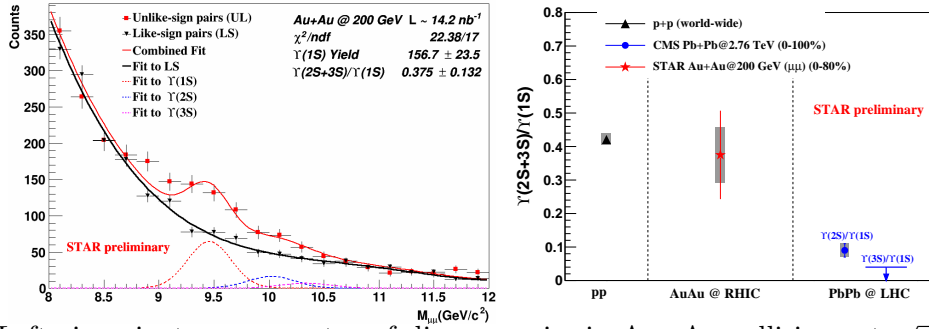
4.2. J/ψ R_{AA} in Au+Au Collisions

J/ψ invariant yields in Au+Au collisions at $\sqrt{s_{NN}} = 200$ GeV have been determined using the data recorded with the MTD in 2014. The results (solid points) are shown as a function of p_T for different centrality bins in the left panel of Fig. 4, and are found to be consistent with the STAR published results from the dielectron channel (open points) [17]. The middle (right) panel shows the R_{AA} for $p_T > 0$ (5) GeV/c determined from the MTD data (red stars). Also shown are the results from PHENIX in Au+Au collisions at $\sqrt{s_{NN}} = 200$ GeV (black open circles), as well as the results from ALICE and CMS in Pb+Pb collisions at $\sqrt{s_{NN}} = 2.76$ TeV (blue solid circles). For $p_T > 0$ GeV/c, the STAR results are consistent with the PHENIX results, showing a descreasing trend towards more central collisions, while the ALICE results are almost independent of centrality and significantly higher than those at RHIC in the central collisions. Such a difference can be due to larger regeneration contributions to low p_T J/ψ at the LHC with much higher $c\bar{c}$ yields. At high p_T, the R_{AA} at both RHIC and LHC have a descreasing trend towards more central collisions, and the LHC results are lower than those at RHIC. This is likely due to higher energy density and temperature reached at the LHC, leading to stronger J/ψ dissociation. Two different transport models [18, 19], both including dissociation and regeneration, can qualitatively describe the measured R_{AA}.

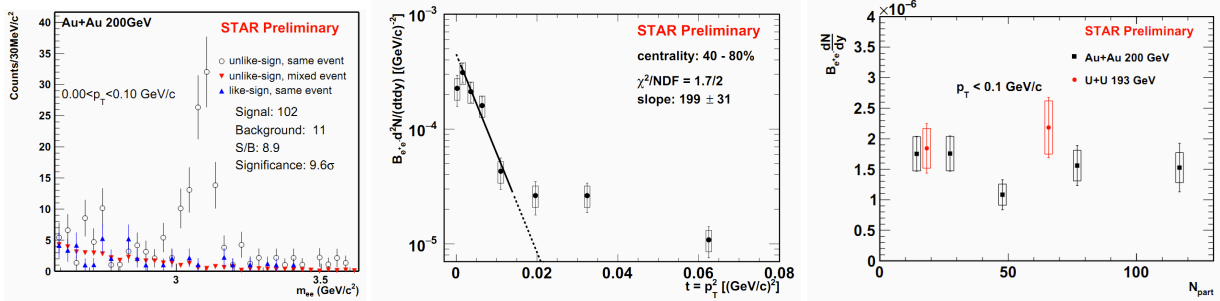### 4.3. Υ Production in Au+Au Collisions

Using the MTD data, STAR has studied Υ production in Au+Au collisions at $\sqrt{s_{NN}} = 200$ GeV. Compared to the dielectron channel, the dimuon channel has the advantage of better invariant mass resolution, thanks to the significantly suppressed bremsstrahlung radiation. Shown in the left panel of Fig. 5 are the invariant mass spectra of dimuon pairs. The unlike-sign (red points) spectrum is fitted to the sum of $\Upsilon(1S)$, $\Upsilon(2S)$ and $\Upsilon(3S)$ signal distributions, and $B\bar{B}$, Drell-Yan and combinatorial background distributions. The shapes of the Υ signal distributions are Gaussian functions with means fixed to the PDG values, and widths determined from detector simulations. The shape of $B\bar{B}$ and Drell-Yan background is determined from PYTHIA6.416 [20]. Both the shape and normalization of the combinatorial background are obtained by fitting the like-sign (black points) spectrum. Shown in the right panel are the ratio of the excited Υ state yield with respect to the ground state yield, obtained from the abovementioned fit, the world-wide p+p data, and CMS measurements in Pb+Pb collisions at $\sqrt{s_{NN}} = 2.76$ TeV. An indication of larger $\Upsilon(2S + 3S)/\Upsilon(1S)$ ratio at RHIC than that at the LHC is observed.

4.4. Very Low p_T J/ψ Production in Au+Au and U+U Collisions

An enhancement of very low p_T J/ψ production has been reported in peripheral Pb+Pb collisions at $\sqrt{s_{NN}} = 2.76$ TeV [21]. Such an enhancement has also been observed in peripheral Au+Au (U+U) collisions at $\sqrt{s_{NN}} = 200$ (193) GeV by STAR. Shown in the left panel of Fig. 6 are the invariant mass spectra of dielectron pairs with $p_T < 0.1$ GeV/c in Au+Au collisions. A clear J/ψ peak can be seen for the unlike-sign pairs. The middle panel shows the $t = p_T^2$ spectrum of J/ψ candidates in the 40-80% centrality bin, together with an exponential function fit within $0.002 < t < 0.015$ (GeV/c)^2. The slope of the fitted exponential function, 199±31 (GeV/c)$^{-2}$, is consistent with the expected value for coherent photon-Au nucleus interactions. The measured

Figure 5. Left: invariant mass spectra of dimuon pairs in Au+Au collisions at $\sqrt{s_{\mathrm{NN}}} = 200$ GeV; Right: ratio of Υ excited state to the ground state measured in p+p collisions, Au+Au collisions at $\sqrt{s_{\mathrm{NN}}} = 200$ GeV and Pb+Pb collisions at $\sqrt{s_{\mathrm{NN}}} = 2.76$ TeV. See text for details.

Figure 6. Left: invariant mass spectra of dielectron pairs with $p_{\mathrm{T}} < 0.1$ GeV/c in Au+Au collisions at $\sqrt{s_{\mathrm{NN}}} = 200$ GeV; Middle: p_{T}^2 spectrum of J/ψ candidates in Au+Au collisions at $\sqrt{s_{\mathrm{NN}}} = 200$ GeV; Right: invariant yields of J/ψ production with $p_{\mathrm{T}} < 0.1$ GeV/c in Au+Au (U+U) collisions at $\sqrt{s_{\mathrm{NN}}} = 200$ (193) GeV. See text for details.

J/ψ yield with $p_{\mathrm{T}} < 0.1$ GeV/c is independent of centrality between 30-80% and consistent between Au+Au and U+U collisions, as shown in the right panel. Such observations can not be explained by the current photoproduction models and warrents further investigation.

References

[1] L. Adamczyk *et al.* (STAR Collaboration), Phys. Rev. Lett. **113** (2014) 142301.
[2] L. Adamczyk *et al.* (STAR Collaboration), arXiv 1607.07517 (2016).
[3] Technical Design Report: The STAR Heavy Flavor Tracker (2011).
[4] L. Ruan *et al.*, J. Phys. G: Nucl. Part. Phys. **36** (2009) 095001.
[5] M. Lomnitz (for the STAR collaboration), these proceedings.
[6] A. Andronica *et al.*, arXiv 1506.03981 (2015).
[7] D. Banerjee *et al.*, Phys. Rev. D **85** (2012) 014510; H. Ding *et al.*, J. Phys. G **38** (2011) 124070.
[8] B. I. Abelev *et al.* (STAR collaboration), Phys. Rev. D **83** (2011) 052006.
[9] R. E. Nelson, R. Vogt, and A. D. Frawley, Phys. Rev. C **87** (2013) 014908.
[10] M. M. Aggarwal *et al.* (STAR collaboration), Phys. Rev. Lett. **105** (2010) 202301.
[11] A. Adare *et al.* (PHENIX collaboration), Phys. Rev. D **82** (2010) 012001.
[12] Y.-Q. Ma, and R. Venugopalan, Phys. Rev. Lett. **113** (2014) 192301.
[13] Y.-Q. Ma, K. Wang, and K.-T. Chao, Phys. Rev. Lett. **106** (2011) 042002.
[14] J. Adam *et al.* (ALICE collaboration), J. High Eenergy Physics **09** (2015) 148.
[15] E. G. Ferreiro and C. Pajares, Phys. Rev. C **86** (2012) 034903; arXiv:1501.03381 (2015).
[16] H. Drescher *et al.*, Phys. Rept. **350** (2001) 93; K. Werner *et al.*, Phys. Rev. C **89** (2014) 064903.
[17] L. Adamczyk *et. al.* (STAR Collaboration), Phys. Lett. B **722** (2013) 55; Phys. Rev. C **90** (2014) 024906.
[18] Y. Liu *et. al.* , Phys. Let. B **678** (2009) 72; K. Zhou *et. al.* , Phys. Rev. C **89** (2014) 054911.
[19] X. Zhao and R. Rapp, Phys. Rev. C 82 064905 (2010); Nucl. Phys. A **859** (2011) 114.
[20] T. Sjostrand, S. Mrenna, P. Skands, JHEP **05** (2006) 026.
[21] J. Adam *et al.* (ALICE collaboration), Phys. Rev. Lett. **116** (2016) 222301.